Noninvasive Ultrasound Imaging of Inflammation Using Microbubbles Targeted to Activated Leukocytes

Jonathan R. Lindner, MD; Ji Song, PhD; Fang Xu, MD; Alexander L. Klibanov, PhD; Kai Singbartl, MD; Klaus Ley, MD; Sanjiv Kaul, MD

Background—Lipid microbubbles used for perfusion imaging with ultrasound are retained within inflamed tissue because of complement-mediated attachment to leukocytes within venules. We hypothesized that incorporation of phosphatidylserine (PS) into the microbubble shell may enhance these interactions by amplifying complement activation and thereby allow ultrasound imaging of inflammation.

Methods and Results—In 6 mice, intravital microscopy of tissue necrosis factor-α–treated cremaster muscle was performed to assess the microvascular behavior of fluorescein-labeled lipid microbubbles with and without PS in the shell. Ten minutes after intravenous injection, microbubble attachment to leukocytes within inflamed venules was greater for PS-containing than for standard lipid microbubbles (20 ± 4 versus 10 ± 3 per 20 optical fields, $P<0.05$). The ultrasound signal from retained microbubbles was assessed in the kidneys of 6 mice undergoing renal ischemia-reperfusion injury and in 6 control kidneys. The signal from retained microbubbles in control kidneys was low (<2.5 video intensity units) for both agents. After ischemia-reperfusion, the signal from retained microbubbles was 2-fold higher for PS-containing than for standard lipid microbubbles (18 ± 6 versus 8 ± 2 video intensity units, $P<0.05$). An excellent relation was found between the ultrasound signal from retained microbubbles and the degree of renal inflammation, assessed by tissue myeloperoxidase activity.

Conclusions—We conclude that noninvasive assessment of inflammation is possible by ultrasound imaging of microbubbles targeted to activated leukocytes by the presence of PS in the lipid shell. **(*Circulation*. 2000;102:2745-2750.)**

Key Words: echocardiography ■ inflammation ■ leukocytes

Inflammation is a common pathophysiological process in innumerable disease states. A noninvasive imaging method capable of routinely assessing inflammation in vivo would be invaluable as a diagnostic test and for assessing response to therapy.

Gas-filled, encapsulated microbubbles are currently used to assess tissue microvascular perfusion during ultrasound imaging. To satisfy the requirements of a flow tracer, these microbubbles have been designed to possess rheological properties similar to those of red blood cells and normally transit through the microcirculation unimpeded.[1,2] We have recently shown, however, that microbubbles with shells composed of albumin or lipid can bind to activated neutrophils and monocytes[3] and are thereby retained within the microcirculation of inflamed or injured tissues.[4] Within minutes of binding, most microbubbles are phagocytosed, yet they remain acoustically active, so their ultrasound signal in inflamed tissue may be detected after clearance of circulating microbubbles from the blood pool.[3]

The signal intensity from microbubbles retained in regions of inflammation is low because of the relatively small proportion of microbubbles that interact with leukocytes within venules[3,5] and of viscoelastic damping of microbubbles once they are phagocytosed.[3] Amplification of this signal may be possible if microbubble avidity for activated leukocytes could be increased. Attachment of lipid microbubbles to activated leukocytes is mediated largely by serum complement.[4] Opsonization may potentially be enhanced by incorporation of certain moieties in the lipid microbubble shell that amplify complement activation. Prior studies investigating the influence of lipid content on liposome behavior have demonstrated that incorporation of phosphatidylserine (PS) into the membrane accelerates complement activation[6–8] and promotes liposome attachment to monocyte-derived cells.[8–10]

In the present study, we hypothesized that the presence of PS in the lipid shells of microbubbles would enhance their microvascular retention in inflamed tissue. Intravital micros-

Received May 17, 2000; revision received June 20, 2000; accepted June 21, 2000.

From the Cardiovascular Division (J.R.L., F.X., S.K.) and the Department of Biomedical Engineering (J.S., K.S., K.L., S.K.), University of Virginia School of Medicine, Charlottesville; Mallinckrodt Inc (A.L.K.), St Louis, Mo; and the Klinik und Poliklinik für Anästhesiologie und Operative Intensivmedizin (K.S.), Westfälische Wilhelms-Universität, Münster, Germany.

Correspondence to Jonathan R. Lindner, MD, Box 158, Cardiovascular Division, University of Virginia Medical Center, Charlottesville, VA 22908. E-mail jlindner@virginia.edu

Circulation **is available at http://www.circulationaha.org**

copy was used to quantify the extent of interactions between leukocytes and lipid microbubbles with and without PS in their shells. The potential application of PS-containing microbubbles for the assessment of inflammation using noninvasive ultrasound imaging was tested in mice undergoing ischemia-reperfusion of the kidney.

Methods

Microbubbles

Microbubbles with lipid shells (MP1950, Mallinckrodt Inc) were prepared by sonication of decafluorobutane gas with aqueous dispersion of 1 mg/mL poly(ethyleneglycol) stearate (Sigma Chemical Co) and 2 mg/mL distearoyl phosphatidylcholine (Avanti Polar Lipids) in normal saline. Microbubbles containing PS (MP1950-PS, Mallinckrodt Inc) were prepared by addition of 0.3 mg/mL distearoyl-PS (Avanti Polar Lipids) to the dispersion. The mean diameters for MP1950 and MP1950-PS were similar (3.2 ± 0.4 versus 3.2 ± 0.6 μm, $P=0.86$).

Flow Cytometry

Binding of FITC–labeled annexin V to the microbubble shell was used to confirm the presence of PS.[11] MP1950 and MP1950-PS microbubbles (2×10^7) were placed in 200 μL of 10 mmol/L HEPES, 140 mmol/L NaCl, and 2.5 mmol/L $CaCl_2$ (pH 7.4). Half of the microbubble suspension was used as a control, and the other half was incubated with FITC–annexin V conjugate (Molecular Probes, Inc) for 15 minutes. Microbubbles were washed and analyzed in triplicate (1×10^5 events for each) on a FACSCalibur (Becton Dickinson). Data were displayed as histograms of green fluorescence intensity. Positive staining for FITC-conjugated annexin V was defined as appearance of microbubbles within a fluorescence intensity gate that excluded 99% of the control microbubbles.

Animal Preparation

The study protocol was approved by the animal research committee at the University of Virginia. Fifteen wild-type C57BL/6 mice (24 to 30 g) were anesthetized with an intraperitoneal injection (12.5 μL/g) of a solution containing ketamine hydrochloride (10 mg/mL), xylazine (1 mg/mL), and atropine (0.02 mg/mL). Body temperature was maintained at 37°C with a heating pad. Anesthesia was maintained with intravenous administration of 0.1 mg pentobarbital approximately every 45 minutes as needed.

Intravital Microscopy

In 6 mice, cremaster muscle inflammation was produced by intrascrotal injections of 0.5 μg murine TNF-α (Genzyme Corp) in 0.2 mL saline. Two hours later, the animal was anesthetized, and the jugular veins were cannulated for administration of microbubbles and drugs. The right or left cremaster muscle was exteriorized through a scrotal incision and prepared for intravital microscopy. A longitudinal incision was made in the muscle, and the edges were secured to a translucent pedestal. The preparation was superfused continuously with isothermic bicarbonate-buffered saline. Microscopic observations were made with an Axioskop2-FS microscope (Carl Zeiss, Inc) with a saline-immersion objective (SW 40/0.8 numerical aperture). Fluorescent epi-illumination was performed with a 460- to 500-nm excitation filter. Video recordings were made with a high-resolution CCD camera (C2400, Hamamatsu Photonics) connected to an S-VHS recorder (S9500, JVC).

Microbubbles were fluorescently labeled by addition of a fluorescent lipid probe with a peak excitation wavelength of 484 nm (Molecular Probes) before sonication. Intravenous injections of 1×10^7 fluorescent MP1950 or MP1950-PS microbubbles were made in random order separated by 20-minute intervals. Two and 10 minutes after each injection, 20 optical fields encompassing a single venular system with diameters of 25 to 40 μm were observed under fluorescent epi-illumination to determine the number of retained microbubbles. The same venular segments were observed for each injection.

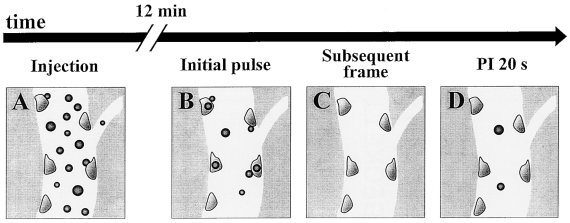

Figure 1. Schematic of ultrasound imaging protocol used to detect microbubbles retained in a region of inflammation. Each panel represents a venule containing adhered leukocytes. See text for details.

Different segments in the venular system were recorded under transillumination at various times during the protocol to determine the number of adherent leukocytes, which were defined as those that did not move for >30 seconds.[12] Leukocyte adhesion was expressed per venular surface area, calculated from offline measurements of vessel diameter and length. In these same venular segments, centerline blood velocities were measured with a dual-slit photodiode (CircuSoft Instrumentation) and converted to mean blood velocities (V_b) by multiplication by 0.625.[13] Shear rates (γ_w) were determined by $\gamma_w=2.12(8\ V_b)/d$, where d is the vessel diameter and 2.12 is a correction factor for the shape of the velocity profile.[14]

Renal Ischemia and Reperfusion

In 6 mice, either the right or left kidney was exposed with a dorsal midline skin incision and paramedian opening of the retroperitoneal space. A hemostatic microvascular clamp (B-1A, ASSI Corp) was placed on the renal pedicle for 30 minutes. Cessation of renal blood flow and subsequent reperfusion were confirmed by tissue pallor during arterial occlusion and prompt return of tissue color after reflow.[15] The surgical wound was closed in layers, and subcutaneous buprenorphine (0.2 μg/g) was given for analgesia.

Renal Ultrasound

Renal ultrasound was performed in the 6 mice undergoing renal ischemia 2 hours after reflow. Bilateral renal ultrasound was also performed in 3 control mice that did not undergo surgery. Animals were anesthetized, and a catheter was placed in a jugular vein for microbubble administration. Imaging was performed at 3.3 MHz with a linear-array transducer interfaced with an ultrasound system (HDI-5000, ATL Ultrasound). Pulse-inversion imaging was used, which improves microbubble signal-to-noise ratio by transmitting 2 sequential pulses of ultrasound that are phase-inverted by 180° so that summation of the 2 sets of radiofrequency responses results in cancellation of tissue signal but not the nonlinear signals produced by microbubbles.[16] Images were acquired in a paraspinal long-axis view with the transducer fixed in position with a free-standing clamp. A mechanical index of 0.8 was used, and the acoustic focus was placed at the level of the renal pelvis. Gain settings were optimized and held constant. Data were recorded on 1.25-cm videotape with an S-VHS recorder (Panasonic MD830, Matsushita Electric).

Before microbubble injection, baseline images were acquired at a pulsing interval (PI) of 1 second. Ultrasound transmission was then suspended, and 1×10^7 MP1950 or MP1950-PS microbubbles were injected as an intravenous bolus. The basis for the imaging protocol used to detect retained microbubbles is schematically depicted in Figure 1. Immediately after injection, a very high concentration of freely circulating microbubbles in the blood pool is expected (1A). Ultrasound imaging was therefore not resumed until 12 minutes after each injection, when the blood pool concentration of freely circulating microbubbles should be low. The video intensity (VI) in the initial frame on resumption of imaging 12 minutes after injection (1B) should therefore reflect the total tissue concentration of microbubbles (both retained and freely circulating).[3] The VI on the next

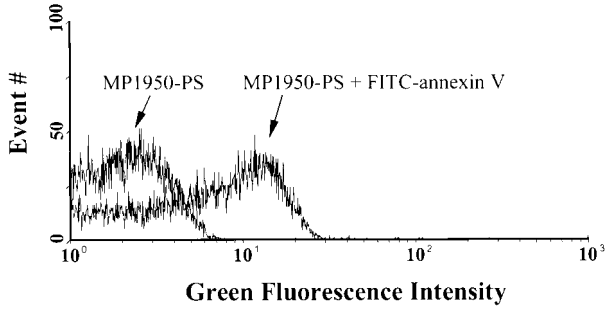

Figure 2. Green fluorescence intensity histograms obtained by flow cytometry of control MP1950-PS microbubbles and MP1950-PS microbubbles incubated with FITC-conjugated annexin V.

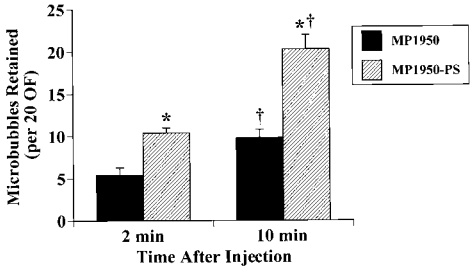

Figure 3. Mean (±SEM) number of MP1950 and MP1950-PS microbubbles retained within cremasteric venules 2 and 10 minutes after intravenous injections of microbubbles. OF indicates optical fields. *$P<0.01$ vs MP1950; †$P<0.05$ vs 2-minute measurement.

few frames (1C) should be lower as a result of destruction of microbubbles by the first and subsequent pulses. After acquisition of several frames, the PI was increased to 20 seconds to allow time for complete replenishment of the beam with microbubbles to assess the signal from any freely circulating microbubbles still present (1D).[17]

Images were analyzed off-line as previously described.[18] Several precontrast frames were averaged and digitally subtracted from the initial frame obtained on resumption of imaging 12 minutes after microbubble administration and from averaged frames obtained at PIs of 1 and 20 seconds. Background-subtracted VI was measured from a region of interest placed around the entire kidney.

Tissue Myeloperoxidase Activity

Renal myeloperoxidase activity was measured to assess tissue neutrophil accumulation.[15] Tissue was homogenized in ice-cold 20 mmol/L potassium phosphate buffer (pH 7.4) and centrifuged at 17 000*g* for 30 minutes at 4°C. The pellet was resuspended in 0.5% hexadecyl-trimethylammonium bromide/10 mmol/L EDTA in 50 mmol/L potassium phosphate (pH 6.0), sonicated, freeze-thawed 3 times, and incubated for 20 minutes at 4°C. After centrifugation, the supernatant was removed and diluted 1:4 in assay buffer. Changes in absorbance were recorded at 460 nm over 5 minutes with a microplate reader (Multiskan MS, Labsystems Inc) and were analyzed with software (Genesis-Lite, Labsystems Inc) resident on a computer workstation. One unit of activity was defined as change in absorbance of 1.0/min at 25°C. Results were given as units of myeloperoxidase activity per gram of protein, determined by BCA assay (Pierce Chemical Co).

Immunohistochemistry

Immunostaining for neutrophils was performed on paraffin-embedded sections of renal tissue. A primary rat anti-mouse antibody (7/4, Serotec Inc) against a polymorphic 40-kDa antigen expressed by neutrophils[19] was placed on the slides overnight at 4°C. The slides were washed, and a biotinylated rabbit anti-rat secondary antibody (Vector Laboratories) was placed on the slides for 1 hour. Staining was performed with a peroxidase kit (ABC Vectastain Elite, Vector Laboratories) and 3,3′-diaminobenzidine chromagen (DAKO). Slides were counterstained with hematoxylin.

Statistical Methods

Data are expressed as mean±SD. Interval comparisons were made with repeated-measures ANOVA. Correlations were made by multiple regression analysis. Differences were considered significant at a value of $P<0.05$ (2-sided).

Results

Flow Cytometry

The histograms of green fluorescence intensity obtained by flow cytometry (Figure 2) illustrate binding of FITC-conjugated annexin V to MP1950-PS microbubbles. Fluorescence intensity was low for the control suspension of MP1950-PS and increased when MP1950-PS was incubated with FITC-conjugated annexin V, confirming the presence of PS in the shell.[11] Compared with MP1950, MP1950-PS was characterized by a higher percentage of microbubbles staining positive for FITC-conjugated annexin V (53±3% versus 16±9%, $P<0.05$) and a greater mean fluorescence intensity (15±4 versus 7±3, $P<0.05$).

Microbubble Retention in Inflamed Venules

The mean blood flow velocity and shear rate in the study venules of the mouse cremaster muscle were 2013±703 μm/s and 987±302 s^{-1}, respectively. The degree of leukocyte adhesion after TNF-α was high (1061±305/mm^2), indicating a pronounced inflammatory response.[4,12] Leukocyte adhesion was not altered by injection of MP1950-PS (1074±291 versus 1037±351/mm^2 for preinjection and postinjection, $P=0.81$).

Microbubble injections were well tolerated in all mice and caused no changes in vessel hemodynamics. On fluorescent epi-illumination, the number of microbubbles retained within inflamed venules 2 minutes after their injection was 2-fold greater for MP1950-PS than for MP1950 (Figure 3). The number of microbubbles retained was even greater at 10 minutes because of their accumulation but remained 2-fold greater for MP1950-PS (Figure 3). Microbubble retention was entirely due to their attachment and eventual phagocytosis by activated leukocytes adherent to the venular endothelium (Figure 4). Freely circulating microbubbles were infrequently observed at the 10-minute interval (<1 microbubble transiting every 5 seconds).

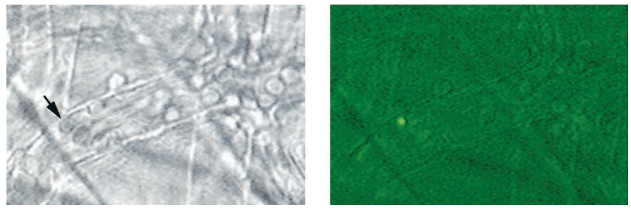

Figure 4. Examples of images obtained by intravital microscopy 2 minutes after injection of MP1950-PS microbubbles. Leukocyte adhesion to venular wall, seen during transillumination, reflects an inflammatory response. Fluorescent epi-illumination revealed a microbubble attached to adhered leukocyte, denoted by arrow in transillumination image.

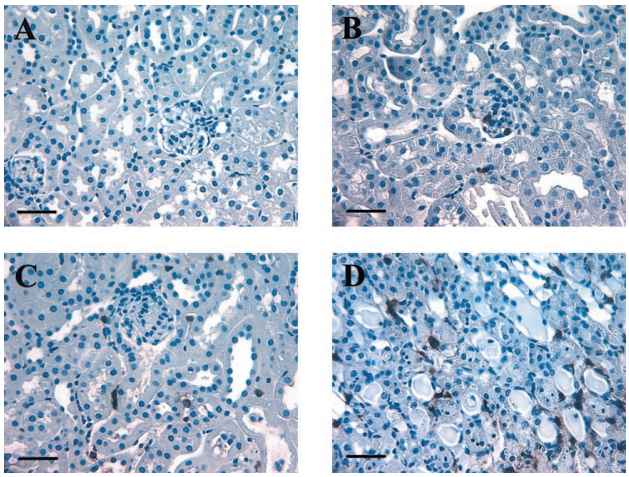

Figure 5. Detection of renal neutrophil infiltration by immunohistochemistry. Neutrophils (stained brown) were absent in cortex of control kidney (A) but were detected within glomeruli (B) and peritubular space (C) after ischemia-reperfusion. Neutrophil infiltration was greatest at cortical-medullary junction (D), where intraluminal debris and some tubular necrosis was also seen. Scale bars=20 μm.

Assessment of Renal Inflammation

Renal myeloperoxidase activity after 30 minutes of warm ischemia and 2 hours of reperfusion was high compared with control kidneys (7.5±3.0 versus 0.5±0.3 U, $P<0.01$). Immunohistology revealed neutrophil infiltration in the glomeruli and in the peritubular regions of the outer medulla and cortex after ischemia-reperfusion (Figure 5B and 5C). Neutrophil infiltration was most abundant at the corticomedullary junction, where intraluminal debris and occasional sloughing of tubular cells were also seen (Figure 5D). These findings were not present in control kidneys (Figure 5A).

The Table shows the background-subtracted VI data obtained by renal ultrasound 12 minutes after microbubble injection. The VI in the initial frame (reflecting both retained and freely circulating microbubbles) in kidneys undergoing ischemia-reperfusion was significantly higher than in control kidneys ($P<0.001$) for both microbubble agents; however, this difference was greater for MP1950-PS than for MP1950 microbubbles ($P<0.01$). In all groups, VI on subsequent frames obtained at a PI of 1 second was very low, indicating destruction of all microbubbles by the first few ultrasound frames. The VI increased minimally when the PI was increased to 20 seconds, indicating the presence of very few freely circulating microbubbles. Examples of background-subtracted color-coded renal ultrasound images are shown in Figure 6. On the initial frame obtained 12 minutes after contrast injection, there is intense opacification of the post-ischemic but not the control kidney. The signal in averaged frames obtained subsequently at a PI of 1 second was very low, indicating destruction of retained microbubbles. This signal remained low at a PI of 20 seconds, indicating a low concentration of freely circulating microbubbles.

Background-Subtracted Video-Intensity Data From Renal Ultrasound 12 Minutes After Microbubble Injection

	Control	Ischemia-Reperfusion
MP1950		
Initial frame	2.3±0.9*	8.5±1.8*†
PI 1 s	0.0±0.4	0.1±0.2
PI 20 s	0.1±0.5	0.4±0.5
MP1950-PS		
Initial frame	2.0±0.7*	19.2±6.8*†‡
PI 1 s	0.0±0.2	1.1±0.6
PI 20 s	0.1±0.2	1.4±1.1

*$P<0.05$ vs corresponding data at PI 1 and 20 seconds.
†$P<0.001$ vs initial frame in control animals.
‡$P<0.01$ vs MP1950 in the ischemia-reperfusion group.

The acoustic signal from retained microbubbles alone was calculated by subtracting the VI at a PI of 20 seconds (reflecting freely circulating microbubbles) from that on the initial frame (reflecting retained and freely circulating microbubbles). The mean acoustic signals from retained microbubbles are depicted in Figure 7 according to the degree of inflammation by renal myeloperoxidase activity. In control kidneys, the myeloperoxidase activity and the signal from retained microbubbles was low. Compared with control kidneys, ischemia-reperfusion–injured kidneys were characterized by much higher ($P<0.001$) myeloperoxidase activity and signal intensity from retained microbubbles. In these kidneys, the mean signal from MP1950-PS was >2-fold higher than MP1950 ($P<0.01$). The correlation between myeloperoxidase activity and the acoustic signal from retained microbubbles in kidneys was linear for MP1950 ($r=0.67$, SEE=6.9, $P<0.05$) and MP1950 ($r=0.69$, SEE=2.7, $P<0.05$) microbubbles. The signal intensity from retained MP1950 microbubbles was not influenced by the order of microbubble injection.

Discussion

We have previously shown that lipid microbubbles are retained within the microcirculation of inflamed tissue because of their attachment to leukocytes adherent to the venular wall.[4] In this study, we have demonstrated that interactions between leukocytes and lipid microbubbles in vivo can be enhanced by altering the shell composition. The presence of PS in the microbubble shell resulted in greater accumulation of microbubbles within inflamed tissue, thereby allowing an accurate assessment of inflammation during ultrasound imaging. This study is the first to demonstrate that contrast ultrasound with intravenous administration of microbubbles can be used to assess inflammation in an organ system.

The molecular mediators of inflammation and toxic products of infiltrating leukocytes have been implicated in tissue damage and organ dysfunction in innumerable disease states. Recently, noninvasive imaging techniques such as computed tomography, magnetic resonance, and ultrasound have been used to detect anatomic alterations associated with inflammation (such as edema). This information is limited, however, by the lack of specificity and inability to discriminate acute from chronic changes. Radionuclide imaging has also been used to evaluate issue inflammation by use of ^{111}In- or ^{99m}Tc-labeled leukocytes, which accumulate in inflamed tis-

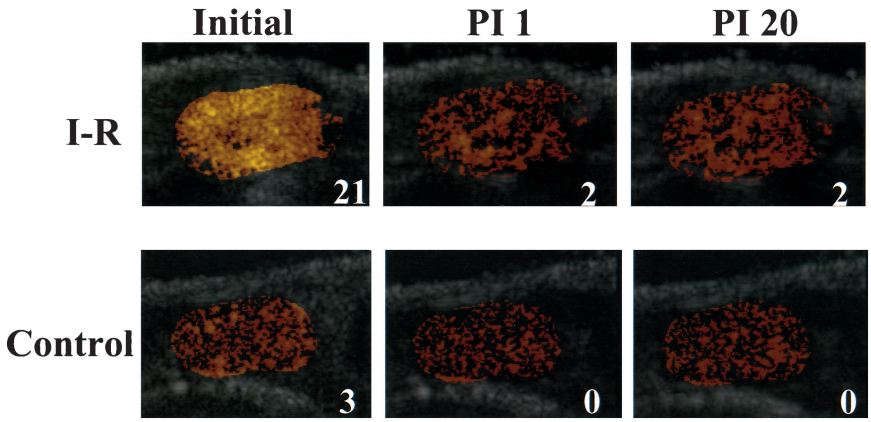

Figure 6. Background-subtracted color-coded ultrasound images of a kidney 2 hours after ischemia-reperfusion (I-R) injury (top) and a control kidney (bottom). Images were obtained 12 minutes after injection of MP1950-PS and include initial frame obtained on resumption of imaging and averaged frames obtained at a PI of 1 and 20 seconds. Background-subtracted VI values from entire kidney are shown in lower right corner of each panel. In I-R kidney, VI on initial frame was high, whereas VI was low on subsequent frames obtained at a PI of 20 seconds, indicating retention of microbubbles within microcirculation at a time when concentration of freely circulating microbubbles was low.

sue, and gallium-67 citrate, which extravasates and is retained in regions of increased capillary permeability.[20–22] Widespread application of these techniques has been limited by the complicated and time-consuming protocols, expense, high radiation burden, and nonspecific tracer uptake in different organ systems.[20,21] An easier and less expensive imaging technique that can routinely and repetitively assess inflammation would therefore be valuable in the clinical setting.

We have recently demonstrated that lipid microbubbles are retained within inflamed tissue because of their complement-mediated attachment to activated leukocytes adherent to the venular endothelial surface.[4] The percentage of circulating microbubbles that are retained is small, however, complicating their detection in tissue.[3,5] In the present study, we hypothesized that microbubble retention could be amplified by incorporating certain lipid moieties in the microbubble shell.

The concept of using PS in the shells of microbubbles was based on prior experience with liposomes, which also undergo opsonization. The presence of PS in liposomes has been shown to accelerate their uptake by phagocytic mononuclear cells[10] and their clearance from the circulation by the reticuloendothelial system.[8,9] Likewise, red blood cells are rapidly cleared from the circulation when the normal mechanisms for sequestering PS to inner cell membrane fail, resulting in translocation of PS to the outer surface.[23] Enhanced uptake of liposomes and red blood cells in these

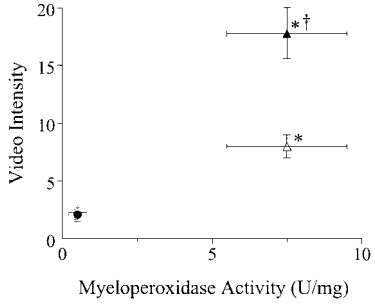

Figure 7. Relation between mean (±SEM) tissue myeloperoxidase activity and VI from MP1950 (open symbols) and MP1950-PS (solid symbols) microbubbles retained within control (circles) and ischemic-reperfused (triangles) kidneys. *$P<0.05$ vs control data for both myeloperoxidase activity and VI; †$P<0.05$ vs MP1950 for VI data.

circumstances is due primarily to enhanced activation of serum complement by either the classic or alternative pathway.[6–8,23] In our present study, intravital microscopy revealed a 2-fold increase of microbubble retention within inflamed tissue by incorporating PS into the microbubble shell.

Whether increased retention of PS-containing microbubbles significantly influenced the ultrasound signal in inflamed tissue imaged in vivo was investigated in a model of renal ischemia-reperfusion injury in mice. Renal inflammation after 30 minutes of warm ischemia and 2 hours of reperfusion was confirmed on immunohistology by neutrophil infiltration in the cortex and especially in the outer rim of the medulla, where expression of proinflammatory cytokines is highest after ischemia-reperfusion.[24] The degree of inflammation was quantified by myeloperoxidase activity,[15] which was markedly elevated after ischemia-reperfusion injury compared to control kidneys. In postischemic kidneys, the ultrasound signal from retained MP1950-PS microbubbles was 2-fold greater than that found with MP1950. A linear relation was found between the extent of inflammation by myeloperoxidase activity and by ultrasound signal from retained MP1950-PS microbubbles.

Although our studies confirm that the presence of PS in the shell of microbubbles enhances their retention in inflamed tissue, we did not necessarily demonstrate that this effect was due entirely to amplification of complement activation. Complement-independent mechanisms for stimulated uptake of PS-containing particles or cells has recently been demonstrated. These mechanisms include direct interactions with scavenger receptors,[25,26] thrombospondin-mediated binding to α_v-integrins,[27] or binding of autologous proteins such as β_2-glycoprotein 1 that facilitate phagocytosis.[28] We also did not directly assess any time-dependent influence of MP1950-PS on the inflammatory response. There were no effects, however, of MP1950-PS on the mean number of leukocytes or the extent of MP1950 attachment to leukocytes, implying little potentiation of the inflammatory response.

Retention of microbubbles as a marker of injury in humans has so far been demonstrated only with direct arterial injections of microbubbles into the myocardium immediately after cardioplegic arrest.[29] Our present results are encouraging that intravenously administered microbubbles may be used for this purpose. In this study, optimization of the signal-to-noise

ratio for phagocytosed microbubbles was necessary. This was done with a novel imaging method that greatly suppresses tissue signal[16] and by acquisition of images late after microbubble injection, which allowed clearance of almost all freely circulating microbubbles from the blood pool, confirmed by intravital microscopy and VI measurements at a long PI.

This study indicates that ultrasound detection of microbubbles retained by activated leukocytes may provide a method for noninvasively assessing the spatial distribution and severity of inflammation. By changing the lipid composition of the microbubble shell, we have increased the avidity of lipid microbubbles for activated leukocytes and thereby enhanced the signal generated during ultrasound imaging of inflamed tissues. The clinical importance of these observations is underscored by the consideration that compared with the radionuclide imaging techniques discussed earlier, ultrasound examination is inexpensive, can be performed rapidly and at the bedside, is widely available, and has a better spatial resolution. Furthermore, the ability to target microbubbles to activated leukocytes in inflamed tissue may also be important for the potential application of microbubbles as vehicles for drug or gene delivery to regions of inflammation.

Acknowledgments

This study was supported by grants HL-03810 (J.R.L), HL-64381 (K.L), and HL-48890 (S.K.) from the National Institutes of Health, Bethesda, Md, and a Beginning Grant-in-Aid (J.R.L.) from the American Heart Association, Mid-Atlantic Affiliate, Baltimore, Md. The authors are grateful to John Sanders for assistance with histology and to Peter Rasche for his assistance with microbubble preparation.

References

1. Keller MW, Segal SS, Kaul S, et al. The behavior of sonicated albumin microbubbles within the microcirculation: a basis for their use during myocardial contrast echocardiography. *Circ Res*. 1989;65:458–467.
2. Jayaweera AR, Edwards N, Glasheen WP, et al. In vivo kinetics of air-filled albumin microbubbles during myocardial contrast echocardiography: comparison with radiolabeled red blood cells. *Circ Res*. 1994;74:1157–1165.
3. Lindner JR, Dayton PA, Coggins MP, et al. Non-invasive imaging of inflammation by ultrasound detection of phagocytosed microbubbles. *Circulation*. 2000;102:531–538.
4. Lindner JR, Coggins MP, Kaul S, et al. Microbubble persistence in the microcirculation during ischemia-reperfusion and inflammation: integrin- and complement-mediated adherence to activated leukocytes. *Circulation*. 2000;101:668–675.
5. Lindner JR, Ismail S, Spotnitz WD, et al. Albumin microbubble persistence during myocardial contrast echocardiography is associated with microvascular endothelial glycocalyx damage. *Circulation*. 1998;98:2187–2194.
6. Conn A, Cullis PR, Devine DV. The role of surface charge in the activation of the classical and alternative pathways of complement by liposomes. *J Immunol*. 1991;146:4234–4241.
7. Comis A, Easterbrook-Smith SB. Inhibition of serum complement haemolytic activity by lipid vesicles containing phosphatidylserine. *FEBS Lett*. 1986;197:321–327.
8. Devine DV, Wong K, Serrano K, et al. Liposome-complement interactions in rat serum: implications for liposome survival studies. *Biochim Biophys Acta*. 1994;1191:43–51.
9. Liu D, Liu F, Song YK. Recognition and clearance of liposomes containing phosphatidylserine are mediated by serum opsonin. *Biochim Biophys Acta*. 1995;1235:140–146.
10. Allen TM, Austin GA, Chonn A, et al. Uptake of liposomes by cultured mouse bone marrow macrophages: influence of liposome composition and size. *Biochim Biophys Acta*. 1991;1061:56–64.
11. Tait JF, Gibson D. Phospholipid binding of annexin V: effects of calcium and membrane phosphatidylserine content. *Arch Biochem Biophys*. 1992;298:187–191.
12. Jung U, Norman KE, Scharffetter-Kochanek K, et al. Transit time of leukocytes rolling through venules controls cytokine-induced inflammatory cell recruitment in vivo. *J Clin Invest*. 1998;102:1526–1533.
13. Lipowski HH, Zweifach BW. Application of the "two-slit" photometric technique to the measurement of microvascular volumetric flow rates. *Microvasc Res*. 1978;15:93–101.
14. Reneman RS, Woldhuis B, oude Egbrink MGA, et al. Concentration and velocity profiles of blood cells in the microcirculation. In: Hwang NHC, Turitto VT, Yen MRT, eds. *Advances in Cardiovascular Engineering*. New York, NY: Plenum; 1992:25–40.
15. Singbartl K, Green SA, Ley K. Blocking P-selectin protects from ischemia/reperfusion induced acute renal failure. *FASEB J*. 2000;14:48–54.
16. Simpson DH, Burns PN. Pulse inversion doppler: a new method for detecting non-linear echoes from microbubble contrast agents. *Proc IEEE Ultrasonics Symp*. 1997;1597–1600.
17. Wei K, Jayaweera AR, Firoozan S, et al. Quantification of myocardial blood flow with ultrasound-induced destruction of microbubbles administered as a constant venous infusion. *Circulation*. 1998;97:473–483.
18. Jayaweera AR, Sklenar J, Kaul S. Quantification of images obtained during myocardial contrast echocardiography. *Echocardiography*. 1994;11:385–396.
19. Hirsch S, Gordon S. Polymorphic expression of a neutrophil differentiation antigen revealed by a monoclonal antibody 7/4. *Immunogenetics*. 1983;18:229–239.
20. Weiner RE, Thakur ML. Imaging infection/inflammations. *Q J Nucl Med*. 1999;43:2–8.
21. van der Laken CJ, Boerman OC, Oyen WJG, et al. Scintigraphic detection of infection and inflammation: new developments with special emphasis on receptor interaction. *Eur J Nucl Med*. 1998;25:535–546.
22. Seabold JE, Palestro CJ, Brown ML, et al. Procedure guideline for gallium scintigraphy in inflammation. *J Nucl Med*. 1997;38:994–997.
23. Wang RH, Phillips G, Medof ME, et al. Activation of the alternative complement pathway by exposure of phosphatidylethanolamine and phosphatidylserine on erythrocytes from sickle cell disease patients. *J Clin Invest*. 1993;92:1326–1335.
24. Daemen MARC, van de Ven MWCM, Hineman E, et al. Involvement of endogenous interleukin-10 and tumor necrosis factor-α in renal ischemia-reperfusion injury. *Transplantation*. 1999;67:792–800.
25. Rigotti A, Acton SL, Krieger M. The class B scavenger receptors SR-BI and CD36 are receptors for anionic phospholipids. *J Biol Chem*. 1995;270:16221–16224.
26. Fadok VA, Warner ML, Bratton DL, et al. CD36 is required for phagocytosis of apoptotic cells by human macrophages that use either a phosphatidylserine receptor or the vitronectin receptor. *J Immunol*. 1998;161:6250–6257.
27. Savill J, Hogg N, Ren Y, et al. Thrombospondin cooperates with CD36 and the vitronectin receptor in macrophage recognition of neutrophils undergoing apoptosis. *J Clin Invest*. 1989;90:1513–1522.
28. Balasubramanian K, Schroit AJ. Characterization of phosphatidylserine-dependent β_2-glycoprotein I macrophage interactions. *J Biol Chem*. 1998;273:29272–29277.
29. Bayfield M, Lindner JR, Kaul S, et al. Deoxygenated blood minimizes adherence of sonicated albumin microbubbles during cardioplegic arrest and after blood reperfusion: experimental and clinical observations with myocardial contrast echocardiography. *J Thorac Cardiovasc Surg*. 1997;113:1100–1108.